CPC(HEP & NP), 2009, **33**(9): 711—716 **Chinese Physics C** Vol. 33, No. 9, Sep., 2009

Systematic impact of spent nuclear fuel on θ_{13} sensitivity at reactor neutrino experiment*

AN Feng-Peng(安丰鹏)[1)] TIAN Xin-Chun(田新春)[2)] ZHAN Liang(占亮)[3)] CAO Jun(曹俊)[4)]

(Institute of High Energy Physics, Chinese Academy of Sciences, Beijing 100049, China)

Abstract Reactor neutrino oscillation experiments, such as Daya Bay, Double Chooz and RENO are designed to determine the neutrino mixing angle θ_{13} with a sensitivity of 0.01—0.03 in $\sin^2 2\theta_{13}$ at 90% confidence level, an improvement over the current limit by more than one order of magnitude. The control of systematic uncertainties is critical to achieving the $\sin^2 2\theta_{13}$ sensitivity goal of these experiments. Antineutrinos emitted from spent nuclear fuel (SNF) would distort the soft part of energy spectrum and may introduce a non-negligible systematic uncertainty. In this article, a detailed calculation of SNF neutrinos is performed taking account of the operation of a typical reactor and the event rate in the detector is obtained. A further estimation shows that the event rate contribution of SNF neutrinos is less than 0.2% relative to the reactor neutrino signals. A global χ^2 analysis shows that this uncertainty will degrade the θ_{13} sensitivity at a negligible level.

Key words θ_{13}, reactor neutrino experiment, spent nuclear fuel, sensitivity

PACS 14.60.Pq, 14.60.-z

1 Introduction

Recent discoveries in neutrino oscillation have unequivocally demonstrated that neutrinos are massive and thus can mix. This intriguing phenomenon depends on two neutrino mass differences (Δm^2_{21}, Δm^2_{32}), three mixing angles ($\theta_{12}, \theta_{23}, \theta_{13}$) and one CP phase δ. The neutrino mass differences and two of the mixing angles have been measured with reasonable precision while the third mixing angle, θ_{13}, has not been determined; the current experimental upper bound is $\sin^2 2\theta_{13} < 0.17$ at 90% C.L. for the nominal value of the mass-squared difference $\Delta m^2_{31} = 2.5\times10^{-3}$ eV^2[1]. A non-zero value of θ_{13} is crucial to measure the CP phase and determine the neutrino mass hierarchy with the next generation of neutrino experiments. Neutrinos from reactors have played an important and decisive role in the early history of neutrino oscillations, which have the potential of uniquely determining θ_{13} at a low cost and in a timely fashion.

The reactor neutrino oscillation experiment was designed to detect reactor $\bar{\nu}_e$'s via the inverse beta-decay reaction

$$\bar{\nu}_e + p \rightarrow e^+ + n\,. \tag{1}$$

The positron annihilated almost immediately with an atomic electron, yielding two 0.511 MeV gamma rays; the neutron was captured later resulting in another emission of gamma rays. The signature is delayed coincidence between the prompt e^+ signal and the signal from the neutron capture. The measured quantity is the survival probability for $\bar{\nu}_e \rightarrow \bar{\nu}_e$ which is given by

$$P_{\bar{\nu}_e\rightarrow\bar{\nu}_e} \approx 1 - \sin^2 2\theta_{13}\sin^2\left(\frac{1.27\Delta m^2_{31}L}{E}\right), \tag{2}$$

where E is the antineutrino energy and L is the distance from antineutrinos production to detection.

The value of $\sin^2\theta_{13}$ can be extracted by comparing the observed antineutrino rate and energy spectrum with the predictions of non-oscillation. The

Received 8 January 2009, Revised 26 February 2009

* Supported by China Postdoctoral Science Foundation Funded Project (20070420527), and National Natural Science Foundation of China (10535050)

1) E-mail: anfp@ihep.ac.cn
2) E-mail: tianxc@ihep.ac.cn
3) E-mail: zhanl@ihep.ac.cn
4) E-mail: caoj@ihep.ac.cn

number of detected antineutrinos, $N_{\rm det}$ is given by

$$N_{\rm det}=\frac{N_{\rm p}}{4\pi L^2}\int \epsilon(E)\sigma(E)P_{\bar{\nu}_{\rm e}\to\bar{\nu}_{\rm e}}S(E){\rm d}E\,, \qquad (3)$$

where $N_{\rm p}$ is the number of free protons in the target, $\epsilon(E)$ is the detection efficiency, $\sigma(E)$ is the total cross section of the inverse beta-decay reaction, and $S(E)$ is the differential antineutrino energy distribution at the reactor.

The goal of the next generation precise reactor neutrino experiments such as Daya Bay[2], Double Chooz[3] and RENO[4] is to determine the last unknown neutrino mixing angle θ_{13} with a sensitivity of 0.01—0.03 in $\sin^2\theta_{13}$, an order of magnitude better than the current limit. The control of systematic uncertainties is critical to achieving the $\sin^2 2\theta_{13}$ sensitivity goal of these experiments. Refs. [5—7] show that the antineutrinos emitted from the spent nuclear fuel (SNF) can distort in a different way the soft part of energy spectra measured in the far and near detectors and thus mimic the oscillation signal. To achieve the challenging goal of the θ_{13} sensitivity in these reactor neutrino experiments, the contribution of SNF neutrinos relative to the reactor produced neutrinos must be known precisely. In this article a detailed calculation of SNF neutrinos is performed taking account of the operation of a typical reactor and the event rate in the detector is obtained. The systematic uncertainty introduced to the θ_{13} sensitivity by SNF neutrinos was studied by a global χ^2 analysis.

2 Spectra, cross section and event yields

The $\bar{\nu}_{\rm e}$ spectrum at reactors was achieved by using the so-called “conversion” approach, and was the superposition of spectra from the beta decaying fission products in the reactor core. The reactors at Daya Bay, Double Chooz or RENO Nuclear Power Plant are of pressurized water reactors (PWR design) as all reactor neutrino experiments have been carried out at PWRs. Fissile materials are continuously consumed while new fissile isotopes are bred from other isotopes in the fuel (mainly ^{238}U) by fast neutrons. Since the neutrino energy spectra are slightly different for the four main isotopes, the fission composition and its evolution over time are therefore critical to the determination of the neutrino flux and energy spectrum.

The beta spectrum from ^{235}U, ^{239}Pu and ^{241}Pu thermal neutron fission fragments was measured online with a magnetic spectrometer[8]. The beta spectrum was then converted into the correlated electron antineutrino spectrum taking into account the Z distribution of the fission products. The antineutrino spectra of ^{238}U which cannot be fissioned by thermal neutrons was obtained by theoretical calculation[9] to estimate the contribution to the $\bar{\nu}_{\rm e}$ spectrum by the ^{238}U fission products. Although these predictions are less reliable than direct measurements, it should be noted that the contribution to the number of fissions, due to this isotope, is quite stable and never higher than 8%. Thus any possible discrepancy between the predicted and the real spectrum should not lead to significant errors.

For a given isotope (j) among the four main isotopes the $\bar{\nu}_{\rm e}$ spectrum can be approximated by a six-parameter function[10]

$${\rm d}N_{\nu}^{\rm j}/{\rm d}E_{\nu}={\rm e}^{a_0+a_1E_{\nu}+a_2E_{\nu}^2+a_3E_{\nu}^3+a_4E_{\nu}^4+a_5E_{\nu}^5}\,, \qquad (4)$$

where the antineutrino energy E_{ν} is in MeV. This recent update improved the spectrum above 7.5 MeV compared with a widely used three-parameter parametrization[11].

Along the year, between periods of refueling, the total effective flux changes with time as the fuel is expended and the isotope relative composition varies. The overall spectrum is at a given time

$$\frac{{\rm d}N_{\nu}}{{\rm d}E_{\nu}}=\sum_{\rm j=isotopes}c_{\rm j}(t)\frac{{\rm d}N_{\nu}^{\rm j}}{{\rm d}E_{\nu}}\,. \qquad (5)$$

The differential cross section at the first order in $1/M$ is given by[12]:

$$\left(\frac{{\rm d}\sigma}{{\rm d}\cos\theta}\right)^{(1)}=\frac{\sigma_0}{2}\left[(f^2+3g^2)+(f^2-g^2)V_{\rm e}^{(1)}\cos\theta\right]\times E_{\rm e}^{(1)}p_{\rm e}^{(1)}-\frac{\sigma_0}{2}\left[\frac{\Gamma}{M_{\rm p}}\right]E_{\rm e}^{(0)}p_{\rm e}^{(0)}\,, \qquad (6)$$

where $f=1$ and $g=1.2601\pm0.0025$ are the vector and axial-vector coupling constants and

$$\sigma_0=\frac{G_{\rm F}^2\cos^2\theta_{\rm C}}{\pi}(1+\Delta_{\rm inner}^R), \qquad (7)$$

where $\Delta_{\rm inner}^R\approx0.024$[13]. Please refer to Ref. [12] for the definition of the positron energy $E_{\rm e}$, the positron momentum $p_{\rm e}$ and the velocity $V_{\rm e}$, etc.

The outer radiative QED corrections of the order of α, including an internal bremsstrahlung contribution, which can be approximated by

$$\sigma_{\rm rad}=\sum_{\rm j}\int_{E_1}^{E_2}11.7\times10^{-3}(E_{\rm e}^{(0)}-m_{\rm e})^{-0.3}\times \sigma_0(f^2+3g^2)E_{\rm e}^{(0)}p_{\rm e}^{(0)}\frac{{\rm d}N_{\nu}^{\rm j}}{{\rm d}E_{\nu}'}{\rm d}E_{\nu}\,, \qquad (8)$$

with the positron energy expressed in MeV is also included.

Thus, we have obtained the final cross-section formula per fission

$$\sigma_{\rm tot}=\sum_{\rm j}\int_{E_1}^{E_2}\int_{\theta_1}^{\theta_2}\left(\frac{{\rm d}\sigma}{{\rm d}\cos\theta'}\right)^{(1)}\frac{{\rm d}N_{\nu}^{\rm j}}{{\rm d}E'_{\nu}}{\rm d}\cos\theta{\rm d}E_{\nu}+\sigma_{\rm rad}\,. \tag{9}$$

The result of the expected total cross section is 5.862×10^{-19} barns/fission $\pm2.7\%$ in the first order with the incorporation of positron angular distribution, weak-magnetism-axial-vector interference correction and radiation correction, which agrees perfectly with the value in Ref. [14]. The parameters used in the calculation and the output of the expected cross section for each isotope are listed in Table 1.

Table 1. Parameters used in the calculation of the neutrino flux and the output of the expected cross-section $\sigma_{\rm i}$ for each isotopes.

isotopes	fission amount $c_{\rm j}$ (%)	$E_{\rm i}$ (MeV/fission)[15]	$\sigma_{\rm i}$ (10^{-19} barns/fission)
^{235}U	53.8	201.7±0.6	6.40±1.9%
^{239}Pu	32.8	210.0±0.9	4.20±2.4%
^{238}U	7.8	205.0±0.9	9.22±10%
^{241}Pu	5.6	212.4±1.0	5.75±2.1%

The neutrino event rate (n_{ν}) per day per ton of liquid scintillator per GW$_{\rm th}$ with a distance $L=1.0\times10^3$ m from the reactor corresponds to a certain average fuel composition and is related to the cross section per fission $\sigma_{\rm tot}$ and the number of target protons $N_{\rm p}$ by

$$n_{\nu}=\frac{24\times3600}{4\pi L^2}\frac{W_{\rm th}}{\langle E_{\rm f}\rangle}N_{\rm p}\epsilon\sigma_{\rm tot}\,. \tag{10}$$

As mentioned above, between periods of refueling, the total effective flux changes with time as the fuel is expended and the isotope relative composition varies. The integral neutrino interaction rate is expected to vary significantly during the reactor fuel cycle. A decrease of about 10% has been forecast for the cross section per fission, as shown in Ref. [16].

3 Spent fuel event rate

In addition to fission, the beta decay of some fission products can also produce antineutrinos with energy higher than the inverse beta decay threshold 1.8 MeV. Most of these fission fragments will soon reach equilibrium, while some others have long lifetimes[5]:

$$\begin{aligned}&^{106}{\rm Ru}(T_{1/2}=372\ {\rm d})\rightarrow{}^{106}{\rm Rh}(T_{1/2}=20{\rm s},\ E_{\rm max}=3.54\ {\rm MeV}),\\&^{144}{\rm Ce}(T_{1/2}=285\ {\rm d})\rightarrow{}^{144}{\rm Pr}(T_{1/2}=17{\rm min},\ E_{\rm max}=3.00\ {\rm MeV}),\\&^{90}{\rm Sr}(T_{1/2}=28.6\ {\rm y})\rightarrow{}^{90}{\rm Y}(T_{1/2}=64{\rm h},\ E_{\rm max}=2.28\ {\rm MeV}).\end{aligned} \tag{11}$$

These long-lived isotopes will accumulate in the core during operational runs. Normally a fuel rod will produce power in the core for 2—3 years and be removed by a manipulator to the water pool near the reactor cores for cooling and shielding. Typically about 1/3 of the burnt-out fuel rods will be removed to the water pool during refuelling every 18 months and after about 5 years each portion will be transported to dry storage far from the reactors. The accumulated spent fuel isotopes in the water pool will continue to contribute to the antineutrino flux via β decay, thus introducing an additional uncertainty to the neutrino flux. The spent fuel data, as well as the realtime running data, will be provided to the Collaboration by the power plant.

For a given isotope i, the neutrino spectrum can be obtained by converting the β spectrum given by Fermi theory under the assumption that both electron and anti-neutrino share the total available energy $E_0^{\rm i}$:

$$S_{\bar\nu}^{\rm i}=E_{\bar\nu}^2(E_0^{\rm i}-E_{\bar\nu})\sqrt{(E_0^{\rm i}-E_{\bar\nu})^2-m_{\rm e}^2c^4}\cdot F(E_0^{\rm i}-E_{\bar\nu},Z^{\rm i}), \tag{12}$$

where $Z^{\rm i}$ is the atomic number of the daughter nucleus, $F(E_0^{\rm i}-E_{\bar\nu},Z^{\rm i})$ is the Fermi correction due to Coulomb interaction in the final state, $E_0^{\rm i}=Q^{\rm i}+m_{\rm e}c^2-E_{\rm exc}^{\rm i}$ where $Q^{\rm i}$ is the released energy of β decay and $E_{\rm exc}^{\rm i}$ is the excitation energy in the daughter nucleus. Generally the neutrino spectrum from Eq. (12) has some discrepancy with the experimental data[17] even taking account of the Fermi correction, especially when Z is large; so we assign a 20% global uncertainty to Eq. (12). The total energy spectrum of the anti-neutrino from SNF can be expressed as the sum of each isotope:

$$S_{\bar{\nu}} = \Sigma_i \alpha^i S^i_{\bar{\nu}}(E_{\bar{\nu}}, E^i_0, Z^i), \tag{13}$$

where α^i is the amplitude of $S^i_{\bar{\nu}}$ which depends on the abundance of isotope i in the SNF and its intensity of radioactivity.

The initial composition of the spent fuel can be precisely calculated if the reactor data are provided. Prior to receiving the detailed data a simple estimation of the concerned isotopes is done by solving the differential equations considering the burn-up effect of fuel, the fission yields of isotopes, the refueling cycle, and the decay of the isotopes themselves. In SNF the isotope composition also evolves over time and is calculated by considering the processes Eq. (11). Fig. 1 shows the time averaged SNF $\bar{\nu}_e$ energy spectrum as well as the detector event rate.

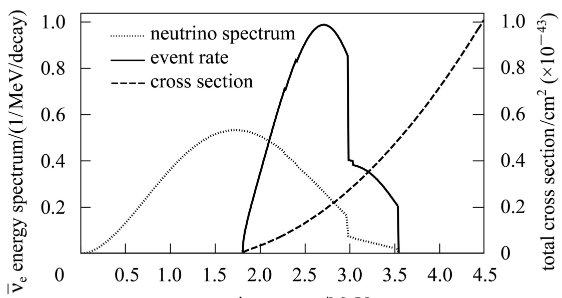

Fig. 1. The 5-year averaged SNF $\bar{\nu}_e$ spectrum (dotted curve), the total inverse beta-decay cross section (dashed curve), and the event rate (solid curve) as a function of antineutrino energy.

The amount of spent fuel directly depends on the thermal power of the reactor, so on average we can compare the neutrino event rate of SNF with the reactor core per GW thermal power. Taking the start time at the beginning of each refueling cycle, and the decay in the spent fuel, the neutrino event rate from these isotopes per day per ton of liquid scintillator per GW_{rmth} with a distance $L=1000$ m from the reactor is given by:

$$n_{\nu}(\text{SNF}) = \frac{24\times 3600}{4\pi L^2}\int_{E_1}^{E_2} N_p \epsilon(t) S_{\bar{\nu}}(t)\sigma^{(0)} \mathrm{d}E_{\nu}\,, \tag{14}$$

where $S_{\bar{\nu}}(t)$ is the total energy spectrum of the SNF isotopes at time t. The neutrino event rate from SNF from Eq. (14) is estimated to be 0.0011, which contributes <0.2% to the signal event rate. Fig. 2 shows the event rate spectrum for SNF neutrinos and reactor signal neutrinos respectively. At the 1.8—3.5 MeV range, the yield increases to 0.3%. As this calculation is based on a simple model without detailed data of the reactor, the uncertainty of SNF composition is estimated as 50% and the event rate uncertainty is estimated to be 100%.

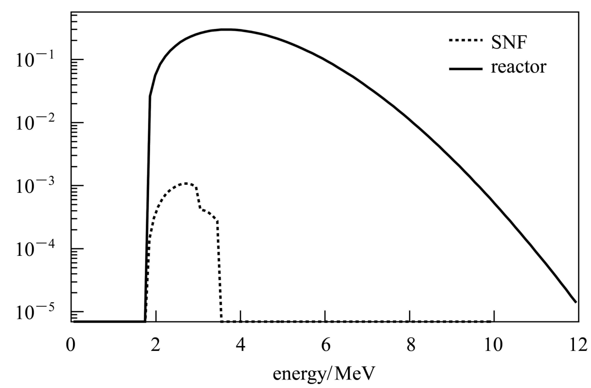

Fig. 2. The detection event rate spectra for SNF (dashed line) neutrinos and reactor signal neutrinos (solid line) in logarithm scale.

4 θ_{13} sensitivity

In this section, we take the Daya Bay reactor antineutrino experiment[2] as an example and substantiate the systematic impact of SNF on the θ_{13} sensitivity using the so-called χ^2 method[18—21]. The systematic errors will be analyzed by constructing the χ^2 function with error correlations introduced naturally. Based on the original Daya Bay χ^2 function[2], we make some modifications to include the impact of SNF and obtain:

$$\chi^2 = \min_{\gamma}\sum_{d=1}^{8}\sum_{i=1}^{N_{\text{bins}}}\frac{\left[M_i^d - T_i^d\left(1+\alpha_c+\sum_r \omega_r^d\alpha_r+\beta_i+\varepsilon_D+\varepsilon^d\right) - S_i^d\left(\sum_s \omega_s^d\alpha_s\right) - \eta_f^d F_i^d - \eta_a^d A_i^d - \eta_h^d H_i^d\right]^2}{T_i^d + (\sigma_{b2b}T_i^d)^2} +$$
$$\frac{\alpha_c^2}{\sigma_c^2} + \sum_r\frac{\alpha_r^2}{\sigma_r^2} + \sum_s\frac{\alpha_s^2}{\sigma_s^2} + \sum_{i=1}^{N_{\text{bins}}}\frac{\beta_i^2}{\sigma_{\text{shp}}^2} + \frac{\varepsilon_D^2}{\sigma_D^2} + \sum_{d=1}^{8}\left[\left(\frac{\varepsilon^d}{\sigma_d}\right)^2 + \left(\frac{\eta_f^d}{\sigma_f^d}\right)^2 + \left(\frac{\eta_a^d}{\sigma_a^d}\right)^2 + \left(\frac{\eta_h^d}{\sigma_h^d}\right)^2\right]. \tag{15}$$

In Eq. (15), d sums over antineutrino detectors, i sums over the energy bins, s is the index of SNF ($s=1,2,\cdots,6$ for 6 reactor cores in the case of Daya Bay experiment) and γ denotes the set of minimization parameters $\{\alpha_c,\ \alpha_r,\ \beta_i,\ \varepsilon_D,\ \varepsilon^d,\ \alpha_s,\ \eta_f^d,\ \eta_a^d,\ \eta_h^d\}$, which are used to introduce different kinds of systematic errors. α_s denotes the systematic error due to SNF-s and other minimization parameters are described in detail elsewhere[2]. The standard deviations of the corresponding parameters are $\{\sigma_c, \sigma_r, \sigma_s, \sigma_{shp}, \sigma_D, \sigma_d, \sigma_f^d, \sigma_a^d, \sigma_h^d\}$. T_i^d is the expected events in the i-th energy bin in detector-d, and M_i^d is the corresponding measured (or simulated) events. F_i^d, A_i^d, and H_i^d are the number of fast neutron, accidental, and ^{9}He/^{9}Li backgrounds respectively. S_i^d is the number of events from SNF and ω_s^d is the weight of neutrino events from SNF-s to detector-d. For each energy bin, there is a statistical error T_i^a and a bin-to-bin systematic error σ_{b2b}. For each point (Δm_{31}^2, $\sin^2 2\theta_{13}$) in the oscillation parameter space, the χ^2 function has to be minimized with respect to the parameters γ.

As discussed in Section 3, the shape error of the SNF $\bar{\nu}_e$ spectrum is less than 20% and the amount error of SNF is 50%—100%. Consequently, we only take into account the amount error of SNF and conservatively set it to be 100%. In Eq. (15), α_s denotes the systematic error due to SNF and its standard deviation σ_s is set to be 100%. We calculate S_i^d based on the shape of the SNF $\bar{\nu}_e$ event rate spectrum shown in Fig. 1 and the total number of detected SNF events by detector-d can be determined by the SNF amount and location of SNF pools. In general, the SNF pool is located no more than 100 m away from the reactor core. In this paper, the systematic uncertainty due to SNF is studied with two different SNF locations. For Case 1, the SNF pools are supposed at the corresponding reactor cores and for Case 2, the SNF pools are located 100 m away from each reactor core where the largest systematic uncertainty is introduced. Actually, the location uncertainty of SNF pools are trivial because we can get the precise location information from the nuclear power plant.

For Case 1 of SNF pools location, the SNF contributes $< 0.2\%$ $\bar{\nu}_e$ events relative to the signal events which are produced by the reactor cores. The signal neutrino event rate from each reactor core has a $\sim 2\%$ uncertainty. The SNF neutrino event rate fluctuation is totally overwhelmed by the signal fluctuation of the reactor cores. Furthermore, the near-far detector setup cancels most of the event rate uncertainties from the reactor cores and SNF at the same level because the reactor cores and SNF have the same location. Fig. 3 shows the sensitivity contours in the $\sin^2 2\theta_{13}$ versus Δm_{31}^2 plane for three years of data taking using χ^2 analysis with and without considering the impact of SNF and the two lines nearly overlap.

For Case 2, though the event rate fluctuation due to SNF is much less than that from the reactor cores, the locations of reactor cores and SNF are different, thus the near-far cancellation is not at the same level. The residual uncertainty from SNF after near-far cancellation is more significant compared with Case 1, therefore the uncertainty from SNF has a much more significant impact on the sensitivity. Fig. 4 shows the sensitivity contours in the $\sin^2 2\theta_{13}$ versus Δm_{31}^2 plane for three years of data taking using χ^2 analysis with and without considering the impact of SNF which has a much larger gap relative to Case 1. However, in the

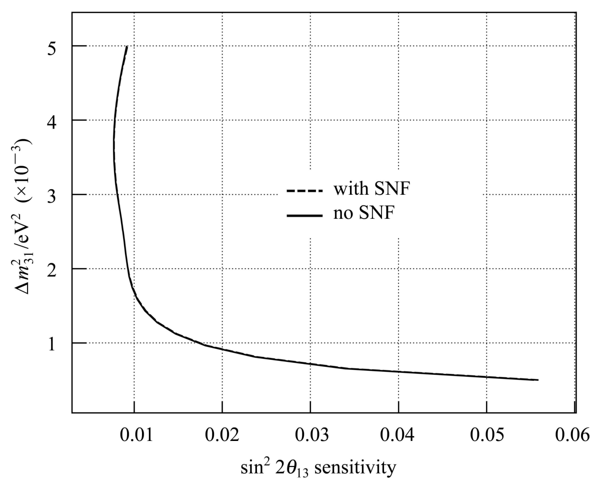

Fig. 3. Sensitivity contours in the $\sin^2 2\theta_{13}$ versus Δm_{31}^2 plane taking into account the impact of SNF (dashed line). The sensitivity contour without considering SNF is also overlayed (solid line) as a reference. Assuming the SNF pools are located at the corresponding reactor cores.

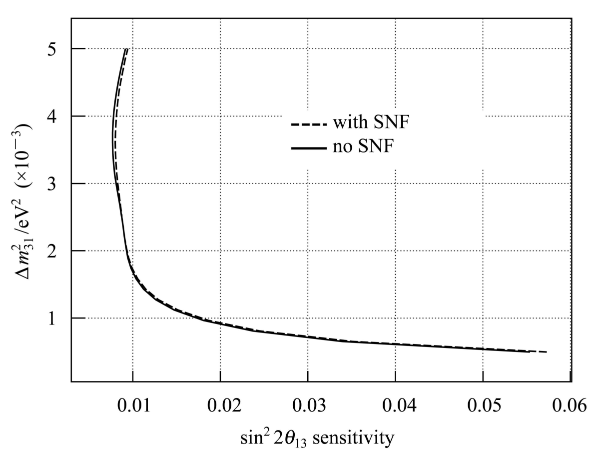

Fig. 4. Sensitivity contours in the $\sin^2 2\theta_{13}$ versus Δm_{31}^2 plane taking into account the impact of SNF (dashed line). The sensitivity contour without considering SNF is also overlayed (solid line) as a reference. Assuming the SNF pools are located 100 m away from the corresponding reactor cores.

3σ confidence region of Δm^2_{31} ($2.0\times10^{-3}\text{eV}^2 < \Delta m^2_{31} < 2.8\times10^{-3}\text{eV}^2$, see Ref. [22]), the impact of SNF is still negligible.

5 Summary

In summary, a detailed calculation of the spent nuclear fuel neutrinos is performed taking account of the operation of a typical reactor. Considering the evolution of some isotopes as neutrino sources in the spent fuel, the event rate in the detector is obtained, and a further estimation shows that the event rate contribution of SNF emitted neutrinos is less than 0.2% relative to the reactor neutrino signals. A global χ^2 analysis shows that SNF impact on θ_{13} sensitivity can be negligible .

References

1 Fogli G L, Lisi E, Marrone A, Palazzo A, Rotunno A M. Phys. Rev. Lett., 2008, **101**: 141801

2 GUO X et al. (Daya Bay Collaboration). arXiv:hep-ex/0701029

3 Ardellier F et al. (Double Chooz Collaboration). arXiv:hep-ex/0606025

4 RENO Collaboration. http://neutrino.snu.ac.kr/RENO/

5 Kopeikin V I, Mikaelyan L, Sinev V. Phys. Atom. Nucl., 2001, **64**: 849

6 Kopeikin V I. Phys. Atom. Nucl., 2003, **66**: 472; Yad. Fiz., 2003, **66**: 500

7 Kopeikin V I, Mikaelyan L, Sinev V. Phys. Atom. Nucl., 2006, **69**: 185

8 von Feilitzsch F, Hahn A A, Schreckenbach K. Phys. Lett. B, 1982, **118**: 162; Schreckenbach K et al. Phys. Lett. B, 1985, **160**: 325; Hahn A A et al. Phys. Lett. B, 1989, **218**: 365; Davis B R, Vogel P, Mann F M, Schenter R E. Phys. Rev. C, 1979, **19**: 2259

9 Vogel P et al. Phys. Rev. C, 1981, **24**: 1543

10 Huber P, Schwetz T. Phys. Rev. D, 2004, **70**: 053011

11 Vogel P, Engel J. Phys. Rev. D, 1989, **39**: 3378

12 Vogel P, Beacom J F. Phys. Rev. D, 1999, **60**: 053003

13 Wilkinson D H. Z. Phys. A, 1994, **348**: 129; Sirlin A. In: Precision Tests of the Standard Model. Edited by Langacker P. Singapore: World Scientific, 1995; Hardy J C, Towne I S. nucl-th/9812036

14 Declais Y et al. Phys. Lett. B, 1994, **338**: 383

15 James M F. J. Nucl. Energy, 1969, **23**: 517

16 Apollonio M et al. Eur. Phys. J. C, 2003, **27**: 331

17 http://ie.lbl.gov/toi/

18 Huber P, Lindner M, Schwetz T, Winter W. Nucl. Phys. B, 2003, **665**: 487; Nucl. Phys. B, 2002, **645**: 3

19 Stump D et al. Phys. Rev. D, 2001, **65**: 014012

20 Fukuda Y et al. Phys. Rev. Lett., 1998, **81**: 1562; Ashie Y et al. hep-ex/0501064

21 Minakata H, Sugiyama H, Yasuda O, Inoue K, Suekane F. Phys. Rev. D, 2003, **68**: 033017; Minakata H, Sugiyama H. Phys. Lett. B, 2004, **580**: 216

22 Maltoni M, Schwetz T, Tortola M A, Valle J W F. New J. Phys., 2004, **6**: 122